Title:

Structures of transcription-translation coupling complexes at each stage of the translation cycle

Authors:

Jing Zhang[1,7], Guoliang Lu[2,7], Wei Zhou[3], Mingxia Yang[1,4], Li Li[2], Huihui Shao[1], Xiaogen Zhou[6], Changbin Chen[1], Richard H. Ebright[5,*], Yue Gao[3,*], Jinzhong Lin[2,*], Chengyuan Wang[1,*]

Affiliations:

1. Shanghai Institute of Immunity and Infection, CAS, Shanghai 200031, China
2. State Key Laboratory of Genetic Engineering, School of Life Sciences, Fudan University, Shanghai 200438, China
3. Department of Pharmaceutical Sciences, Beijing Institute of Radiation Medicine, Beijing, China.
4. University of Chinese Academy of Sciences, Beijing, China
5. Waksman Institute and Department of Chemistry and Chemical Biology, Rutgers University, Piscataway, NJ 08854, USA.
6. College of Information Engineering, Zhejiang University of Technology, Hangzhou, China
7. These authors contributed equally: Jing Zhang, Guoliang Lu

*Correspondence to Y.G. gaoyue@bmi.ac.cn; R.H.E. ebright@waksman.rutgers.edu; J.L. linjinzhong@fudan.edu.cn; C.W. cywang@ips.ac.cn;

Abstract:

Bacterial transcription and translation are frequently linked through a transcribing RNA polymerase following the leading ribosome, a process termed transcription-translation coupling (TTC). Three distinct TTC structures, the “collided expressome” (TTC-A), the “coupled expressome” (TTC-B) and the “long-range coupled expressome” (TTC-LC) have been reported, but the biological significance of all complexes is still subject to uncertainty. Furthermore, all of the ribosomes in the structures are determined in a static state. The underlying translation dynamics within these TTCs remain elusive. Here, we reconstitute the complete active transcription-translation system, using antibiotics and a series of different lengths of mRNAs to trap intermediate coupling states, and determine Cryo-EM structures showing the snapshots for the dynamic reaction trajectory. The results show five states of TTC-B representing the whole stages of the translation elongation cycle. TTC-B is compatible with ribosome conformational changes during translation elongation and coordinates transcription elongation with translation elongation. The results show two distinct TTC-A in translational pre-translocation and translocation intermediate states in which the RNAP becomes unstable as the translation progresses. The results further show that TTC-A is the crucial state where the ribosomes could exert mechanical force on RNAP, leading to the potential transition between TTC-A and TTC-B within mRNA spacer ranging from 7 to 9 codons and suggesting a ribosome-dependent transcription termination within mRNA spacer shorter than 7 codons. The results further show TTC-LC is also compatible with ribosome conformational changes during translation elongation cycle but with less stability compared with TTC-B and shows the potential transition with TTC-B within mRNA spacer of 13 codons. Our results provide a comprehensive blueprint detailing the dynamic interplay of transcription-translation coupling.

Introduction

In bacteria, the absence of a nuclear envelope allows the first ribosome (leading ribosome) to translate mRNA closely coordinated with RNA polymerase (RNAP)[1,2]. This coordination allows for the synchronization of transcription and translation rates by the lead ribosome[3-13]. The physical interactions between these two macromolecular machines are indispensable for both transcription and translation processes, and it has been reported that coupling transcription with translation can regulate gene expression[4,7-9,12,14-21]. It does so by mediating the transcription attenuation[22,23], preventing premature transcription termination[24-27], reactivating halted or paused RNAP[14,19,20], protecting RNA from degradation, and inhibiting the formation of deleterious R-loops[4,28,29].

NusG is crucial in mediating the coordination between transcription and translation in *E. coli.*[3,6,13,30,31]. It is the only transcription factor that is conserved across all domains of life, including bacteria, archaea, and eukaryotes[30,32,33]. NusG facilitates the connection between RNAP and the leading ribosome through the interaction of its N-terminal domain (NTD) with RNAP and the simultaneous engagement of its C-terminal domain (CTD) with ribosomal protein S10 [6,10,31]. NusA, another transcription elongation factor in *E. coli*, can also modulate transcription-translation coupling. While NusA can augment and support the bridging function of NusG, it cannot replace it entirely [34,35].

Using cryo-EM, researchers have recently begun to reveal atomic structures of *E. coli* transcription-translation coupling complexes (TTCs)[35-38]. The insightful results delineate three distinct classes of TTCs. "Collided Expressome" (referred to as TTC-A) are captured with short mRNA spacers between RNAP and the ribosome[35-37]. These complexes are notable for being incompatible with NusG bridging and NusA binding. Molecular modeling suggests that TTC-A would conflict with transcriptional processes in *E.coli*, including elongation, pausing, and termination[35]. "Coupled Expressome" (TTC-B), characterized by mRNA spacers from 8 to 10 codons, depend on NusG and can accommodate NusA[35,37]. Significantly, TTC-B is compatible with the complete transcriptional cycle in *E.coli*[35,37]. "Long-range coupled" or "Loose-coupled Expressome" (TTC-LC) was determined with spacer longer than 12 codons and also depend on NusG[38].

Despite the available TTC structures, several fundamental questions remain unanswered, particularly concerning the dynamic interplay between ribosome movement and RNAP activity during translation elongation. As the ribosome deciphers the nascent mRNA, it undergoes a coordinated choreography of conformational changes -- binding and releasing of translation factors and tRNAs, translocating of the ribosome along the mRNA that further involves ratcheting of the 30S ribosomal subunit by ~9° relative to 50S

subunit and the 30S head swivel by ~20° relative to the body[39-42]. Strikingly, all reported TTCs show ribosomes in a static, non-rotated state with the initiator tRNA bound to the P-site of the ribosome[35-37]. How these dynamic structural changes within the ribosome are accommodated within the coupled complex remains a puzzle.

Another critical question relates to the mechanistic basis of RNAP enhancement by the leading ribosome. The physical link between RNAP and the leading ribosome is postulated to promote transcription elongation by pushing a slow or paused RNAP[14,19,20]. The coupled ribosome was further revealed to be able to terminate the stalled RNAP which was arrested due to template-strand DNA damage[21]. Recently, by reconstituting and tracking an *in vitro* active transcription-translation coupling system, Qureshi and Duss reports that the ribosome slows down while colliding with the RNAP and the ribosome preferentially ends up in the rotated state[43]. They further shows long-range physical coupling could rescue RNAP from frequent pausing[43]. However, the precise mechanism by which the ribosome exerts this mechanical force on RNAP remains obscure.

Finally, the comprehensive understanding of the transcription-translation coupling process and the biological significance of “collided”, “coupled”, and “loose-coupled” TTCs are still subjects of uncertainty. The complete scope and implications of these complex interactions in a cellular context are yet to be fully understood.

Here, to address these critical questions, we reconstitute the complete active transcription-translation system *in vitro*, use a series of different lengths of mRNAs representing the dynamic transcription-translation coupling stages, and determine different coupling structures by using single-particle reconstruction cryo-EM. Our results show the whole snapshots for the dynamic coupling reaction trajectory and unveil that (i) the ribosome within TTC-B is capable of pass-through translocation trajectory, accommodating mRNA with a codon spacer ranging from 7 to 10; NusA and NusG finely tune the RNAP orientations relative to the ribosome, further supporting the functional significance of TTC-B in coupled transcription-translation. (ii) The TTC-A represents a state wherein the ribosome applies mechanical force on RNAP through mRNA, holding the ribosome in the PRE or early CHI state with mRNA having a codon spacer of 7 to 9. (iii) both TTC-A and TTC-B co-exist for spacer length of 7 to 9 codons, suggesting a dynamic conformational equilibrium between them; (iv) With nucleic acid scaffolds that have mRNA spacers shorter than 7 codons, the coupling complex de-couples, the new identified class of ribosomes with extracted RNA, indicates the ribosome-dependent termination as an alternative mechanism for transcription termination. (v) With nucleic

acid scaffolds that have mRNA spacers of 13 codons, we captured TTC-LC, maintaining complete coupling during the translation process. Taken together, our results provide an all-encompassing perspective on dynamic transcription-translation coupling.

Assembly of functional transcription-translation coupling complexes

We reconstituted TTCs using a series of mRNA fragments with different length spacers that annealed to a DNA scaffold, mimicking the elongation complex of an actively transcribing RNA polymerase. The mRNA was deliberately designed to have a codon for phenylalanine following the initiation codon (Figure 1A). We systematically assembled TTCs by incorporating the 70S ribosome, initiator tRNA fMet-tRNA^{fMet}, ternary complex EF-Tu•Phe-tRNA^{Phe}•GTP into RNAP transcription elongation complex (TEC) with different length of mRNA spacers[39,44]. The ternary complex EF-Tu•Phe-tRNA^{Phe}•GTP facilitated the delivery of the elongator tRNA to the A-site of the ribosome. By introducing EF-G with GTP analogs (GDPCP), antibiotics (viomycin and fusidic acid)[45-47], we successfully trapped the TTC with the ribosome positioned at specific translation elongation intermediates and at the post-translocation state (Figures 1B and S1-S3). For each resulting complex, we determined the structures using single-particle reconstruction cryo-EM. A summary of TTC states with specific codon spacer, antibiotics, and resolution shell can be found in Table S1.

Structures of TTC-B in each state of translation elongation cycle

TTC-B, in the presence of NusA and NusG bridging the RNAP and ribosome (NusA-NusG-TTC-B), are obtained with nucleic acid scaffolds having mRNA spacers of 7, 8, 9, or 10 codons (Figure 2A and Table S1). A total number of 27 TTC-B structures were determined (Figures S4 and S5) and could be divided into five distinct TTC-B states (states 1-5), each representing different stages of the ribosome translation elongation cycle (Figures 2A, 2B, S4 and S5, and Table S1). Within each identified state, TTC-B could be further categorized into sub-class based on the relative orientation of RNAP to the ribosome (Figures S4 and S5). The spatial relationship of RNAP to the ribosome and the ribosomes in each state are identical in structures obtained with different spacer lengths of mRNA (Figures S4 and S5). In subsequent sections, we will elaborate on the ribosome elongation states 1 to 5, elucidating the conformational changes of RNAP relative to the ribosome, as mediated by the interactions of NusA and NusG.

In TTC-B state 1, the ribosome adopts a canonical non-rotated conformation (Figure 2A, first panel). High-resolution data clearly reveals the trajectory of mRNA as it emanates from the RNAP transcription

active center and transverses along a positively charged patch on ribosomal proteins uS3 into the mRNA-entrance channel on the ribosome. Eventually, the mRNA forms base paired with the anticodon of the tRNA molecules. Within this conformation, two tRNAs adopt the classical A/A and P/P states, while a tRNA with low occupancy is found in the E-site (Figure 2B, first panel). These observations align with previous studies on translation elongation[39,42,48,49].

The TTC-B states 2 and 3 were captured using viomycin with an mRNA spacer of 9 or 10 codons. In both states, the 30S ribosomal subunit undergoes a rotation relative to the 50S subunit, anchored by EF-G to the sarcin-ricin loop (Figures 2A and S6A). In state 2, the domain IV of EF-G (EF-G pre state, "EF-G pre") is positioned adjacent to the A site of 30S, engaging with the anticodon stem of the A-site tRNA. The acceptor arm of $tRNA^{Phe}$ in the A site is displaced by ~25 Å towards the peptidyl transfer center (PTC), while the deacetylated P-site tRNA transitions to the E site of the 50S subunit, resulting in an A/P* and P/E configuration, respectively (Figure 2B, second panel). In state 3, the domain IV of EF-G (EF-G pre/post state, "EF-G pre/post") moves ~14 Å closer to the anticodon stem of the A-site tRNA (Figure S6B). The conserved loop (residues 507-514 in *E.coli* EF-G) interacts extensively with the anticodon stem-loop of the A site tRNA, leading to a shift of $tRNA^{Phe}$ from A/P* state to A/P state (Figure 2B, third panel).

In state 4, the domain IV of EF-G (EF-G post state, "EF-G post") moves ~18 Å further and takes the A site on the 30S subunit, resulting in the $tRNA^{fMet}$ being in the P/E site (Figures 2B, fourth panel, and S6B). This state was captured using GDPCP, viomycin, or fusidic acid. The TTC-B states 2-4 represent transcription-translation coupling complexes with ribosomes progressing along the translocation trajectory.

In TTC-B state 5, following the translocation of tRNA by one codon, the 30S subunit reverts to the non-rotated state. Domain IV of EF-G occupies the A site, positioning $tRNA^{Phe}$ and $tRNA^{fMet}$ in the P/P and E/E sites, respectively (Figure 2B, fifth panel). This state was captured using GDPCP, viomycin, or fusidic acid. It represents TTCs with the ribosome in the post-translocation state, which is usually followed by the subsequent release of EF-G, and setting the stage for the A site to accommodate an incoming aminoacyl-tRNA, thereby initiating another cycle of translation elongation[39,42,44]. Taken together, the TTC-B state 1-5 represents the whole states of the translation elongation cycle with transcription-translation coupling.

Throughout the translation elongation cycle, the RNAP within the TTC-B engages with the 30S subunit in a flexible yet stable manner. The RNAP densities in all five states of TTC-B are clear, enabling unambiguous rigid-body docking of atomic structures of the transcription elongation complex. The architectures of these five complexes are similar, yet not identical, to previously reported TTC-B structures[35].

In these, NusG bridges RNAP and the ribosome with NusG-N binding to RNAP and NusG-C binding to ribosomal protein uS10 on 30S head; NusA further stabilizes the complexes through its AR2 and NusA-NTD domain binding to RNAP, and its KH1/2 domain interacting with ribosomal protein uS2 and uS5 on the 30S body. Additionally, the RNAP β' ZBD domain interacts with ribosomal protein uS3 (Figures 2A-2D). Comparative analysis of the five TTC-B states provides detailed insights into the conformational dynamics between RNAP and the ribosome during the translation elongation cycle. From TTC-B state 1 to state 2, the 30S subunit rotates ~8.6^{o} (counter-clockwise direction from the top view on 30S), while the RNAP rotates ~7.5^{o} in the same direction in a coordinated manner (as per superposition on 50S, Figure 2C, left). Concurrently, the 30S head domain swivels ~4.4^{o} with RNAP rotating ~9.1^{o} in the same direction (Figure 2C, right). These coupled movements between RNAP and the 30S subunit are fine-tuned by NusG and NusA, which rotate ~11.3^{o} and ~2.2^{o}, respectively (Figure 2C. right). Besides these coupled movements, the RNAP also exhibits a ~12.5^{o} swinging movement relative to 30S throughout the translation elongation cycle (comparing the five states of TTC-B by structure superposition on 30S, Figure 2D). In some states of TTC-B, several subclasses are also discerned (e.g. subclass1, 2, and 3 in state 1 and state 5; subclass1 and subclass2 in state 3 and 4). These subclasses differ by ~15° rotation of RNAP relative to 30S, resulting in the distance between the transcription active center and the ribosome mRNA-entrance portal changes from 79 Å, to 85 Å or 90 Å, respectively (Figure S7). In general, the movements between RNAP and ribosome in TTC-B is relatively free but within a certain range.

The stable yet flexible interactions between RNAP and the ribosome are contingent on the subdomain architecture of NusG and NusA. The NusA protein forms an open-rectangular-frame, termed "pantograph" structure, comprising six domains: NusA-NTD, -S1, -KH1, -KH2, -AR1, and -AR2. NusA-NTD interacts with RNAP αCTD^{II} and can shift by ~22 Å across the five different states. However, the flexible linker connecting NusA-S1 and NusA-NTD (residues 133-139 in *E. coli* NusA) allows NusA-S1 to remain relatively stable with RNAP β FTH. The flexible linkers between the NusA KH2 and AR1 domains (residues 394-403 in *E.coli* NusA), and between the AR1 and AR2 domains (residues 428-435 in *E.coli* NusA), enable the AR2 domain to move with RNAP αCTD^{I} (within a range of ~10 Å) while maintaining the binding of the NusA-KH2 domain with ribosomal proteins uS5 and uS2 (Figures 2D and 2E). NusG, similar to NusA, has a flexible linker (residues 116-128 in *E.coli* NusG) between its NTD and CTD, allowing the NusG-NTD to shift ~26 Å in response to the swinging of RNAP without disturbing the interactions between the NusG-CTD and uS10 (Figures 2D and 2F).

Based on these observations that TTC-B is compatible with ribosome conformational changes during the translation elongation cycle and coordinates transcription elongation with translation elongation, we propose that TTC-B modulates NusG-dependent, NusA-dependent dynamic transcription-translation coupling in *E.coli*.

Structures of TTC-A in early stage of translation elongation cycle

In addition to TTC-B, we also captured two distinct collided coupling states (TTC-A) in a ratchet state[40] with EF-G, the pre-translocation and translocation intermediate, specifically designated as state 2 and state 3. A notable feature of both states is the absence of NusA and the lack of interaction between the NusG-CTD and ribosomal protein uS10, rendering them unable to sustain the canonical TTC-B state (Figure S8). The overall architectures of these states are distinctly different from the previously identified collided coupling state (referred to as TTC-A state 1 for clarity). In TTC-A state 1, the ribosome is in a non-ratcheted conformation, while the action of EF-G propels it into the ratcheted one in TTC-A states 2 and 3. Specifically, in TTC-A state 2, EF-G is in the 'EF-G pre' state, with two tRNAs occupying the A/P* and P/E sites, respectively (Figures 3A left and 3B left). In TTC-A state 3, the 30S subunit is also in a rotated state, with EF-G assuming the 'EF-G pre/post' state and the two tRNAs situated in the A/P and P/E sites, respectively (Figures 3A right and 3B right).

The spatial relationships between RNAP to the ribosome in these newly identified states of TTC-A also contrast with that in the previously characterized “initiation-like” TTC-A state 1[35-37], where RNAP is more flexible and has reduced protein-protein interactions with the 30S subunit. Specifically, RNAP in TTC-A state 2 exhibits a ~2.5^{o} counterclockwise rotation compared to TTC-A state 1 (from the top view, as compared in the two states of TTC-A by structure superposition on the 30S, Figure S8A). From state 2 to state 3, RNAP undergoes further rotation of ~4.1^{o} and shifts ~2.1Å relative to the ribosome (Figure 3C). These RNAP movements are relative to the 30S lead to the disruption of interfaces between RNAP β’ ZBD domain and ribosomal protein S4 (Figure 3D), and between RNAP αI and ribosomal protein S10 (Figure 3E), resulting in a significantly poorer density in these regions of RNAP. Although we reconstituted TTC with varying mRNA spacer lengths (7-10 codons) and different GTP analogs or antibiotics, only TTC-A states 2 and 3 (CHI-states) were captured. This suggests that TTC-A cannot be formed during the later stages of the translation elongation process. Preprint reports that stalled RNAP leads to ribosome slowdown upon collision, and the ribosome preferentially ends up in the rotated state[43]. Our result shows that the ribosome needs to overcome more

difficult conformational changes in TTC-A during the translation elongation cycle compared with TTC-B, thus leading to the slowdown of translation and may more likely end at the rotated states.

Functional relationship between TTC-A and TTC-B

The simultaneous capture of both TTC-A and TTC-B in the presence of a codon spacer ranging from 7 to 9 codons raises intriguing possibilities about potential state transformations during the translation elongation process (Figure 3F). In our earlier work[35], TTC-A was exclusively observed in state 1 using a spacer 7 codons mRNA (Figure 3F, upper panel). However, in this study, both TTC-A and TTC-B were obtained using a spacer 7 codons mRNA, with a near-equal particle distribution of 50.5% for TTC-A and 49.5% for TTC-B (as depicted in Figure 3F, lower panel, and Table S1). As the spacer length of mRNA becomes longer, a higher ratio of TTC-B was captured compared with the previous study. These findings imply that the introduction of translation factors EF-Tu and EF-G might induce a significant remodeling of the overall architecture of TTC, potentially facilitating the transition from TTC-A into TTC-B during translation elongation. Notably, when using a spacer of 9 codons, previous experiments[35] yielded only the TTC-B state (Figure 3F, upper panel), while the current study achieved a simultaneous capture of both TTC-A and TTC-B states. Although TTC-B is dominant (92.5%) in this scenario, the presence of TTC-A (7.5%) is a crucial observation (as depicted in Figures 3F, lower panel and S1). This co-occurrence suggests that even during active transcription translation coupling, as typified by the TTC-B state, translation elongation factors may potentially disrupt the stabilizing interactions mediated by NusA and NusG, thereby leading to a state transition from TTC-B to TTC-A. This transition indicates a dynamic and potentially reversible interaction between the components of the transcription-translation machinery. In light of our observations regarding TTC-A states 2 and 3, we propose a model where RNAP undergoes a counterclockwise rotation during the transition from TTC-A to TTC-B and, conversely, a clockwise rotation during the transition from TTC-B to TTC-A (Figure S8B).

TTC-A may also play a pivotal role in the termination of transcription. Our previous research, employing a nucleic acid scaffold with a mRNA spacer of 5 and 6 codons, yielded exclusively non-rotated TTC-A structures (Figure 3F, upper panel). However, in the current study with the same configuration, where we energized the ribosome with translation elongation factors, we observed a complete absence of TTCs (Figures 3F and S9). Further analysis identified two distinct classes of ribosomes within the same cryo-EM dataset. The first class, displaying no mRNA density around the ribosome's mRNA entry channel, represents what we termed the "un-coupled" ribosome (Figure S10B). These could be free, non-translating ribosomes and are

also observed in other TTC-A datasets with 7 to 9 codon spacers. The second class is more biologically significant and presents robust mRNA density interacting with the positively charged patch of the ribosomal proteins uS3, extending from the mRNA entry channel to the decoding center. We refer to this second class as 'de-coupled' ribosomes (Figure S10A), hypothesizing that they emerge from transcription termination, triggered by the ribosome exerting mechanical force on the TEC, consequently disrupting it and extracting the RNA. The findings of our study suggest that within the transcription-translation coupling complex, the ribosome can promote the termination of TEC as an alternative mechanism for transcription termination. In this scenario, the ribosome, through continuous translation in the TTC-A state, shortens the mRNA length between RNAP and the ribosome to a critical point (7-condon spacer) where the transition from TTC-A to TTC-B is not viable.

New conformations of transcription-translation coupling complex with long-range mRNA

We first obtained the coupling complexes with nucleic acid scaffolds having mRNA spacers of 7, 8, 9, or 10 codons, and then further sought and obtained a new class of TTC-LC with longer spacer length mRNA (13 codons). In this new class of TTC-LC, which is similar with previously reported TTC-LC but with complete different stages of ribosomes[38]. Three states (state1, state3, and state5, Figure S11) of TTC-LC were obtained and two of them (NusA-NusG-TTC-LC state1 and state3) could perform the unambiguous rigid-body docking and further structural model building. The ribosomes in each of the two TTC-LC states is identical to the ones in TTC-B while the RNAP in TTC-LC is further away from the ribosome compared with TTC-B (Figure 4A). A ~100Å, ~18nt mRNA segment connected the RNAP RNA-exit channel and ribosome mRNA entrance portal, running along the surface of NusA-S1, NusA-KH1, and ribosomal protein S3 (Figures 4A and 4B). In all NusA-NusG-TTC-LC states, RNAP and NusG interact with ribosome 30S head, with RNAP β' ZBD contacting NusG and NusG contacting ribosomal proteins S10 (Figure 4B). Different with TTC-B, in NusA-NusG-TTC-LC, RNAP β' ZBD make additional interactions with NusA-S1 domain (Figure 4B). Moreover, in the new class of TTCs, NusA translated ~40Å relative to the ribosome, disrupting the interactions between NusA and ribosome 30S body (involving contacts between NusA-KH1 domain and ribosomal protein S2 and S5). Instead, NusA interacts with mRNA via its KH1 and S1 domains, and only NusG directly connects the RNAP and Ribosome (Figure 4D).

TTC-LC is compatible with ribosome conformational changes during the translation elongation cycle. The ribosomes of TTC-LC represent the whole states of the translation elongation cycle (although some

intermediate states were not determined). Throughout the translation elongation cycle, the RNAP within the TTC-LC engages with 30S subunit in a more flexible manner compared with TTC-B. As NusA was no longer binding with the 30S body, when the ribosome rotated from state1 to state3, RNAP had more dramatic conformational changes compared with the changes in TTC-B (7.1^{o} in TTC-LC versus 2.2^{o} in TTC-B, Figure 4C). Besides the three states of NusA-NusG-TTC-LC classes, two subclasses were obtained in NusA-NusG-TTC-LC (subclass1, and 2 in state1, Figure S12A). Similar to TTC-B, two subclasses differ by ~15° rotation of RNAP relative to 30S, resulting in the distance between the transcription active center and the ribosome mRNA-entrance portal changing from 101Å to 106Å (Figure S12B). In general, the movements between RNAP and ribosome in TTC-LC are relatively more flexible than in TTC-B, but they are also within a certain range.

Potential state transformations may also occur between TTC-LC and TTC-B. With nucleic acid scaffolds having mRNA spacer of 13 codons, NusA-NusG-TTC-B (37.6% in all coupling complexes) could also be obtained (Figure 4A, Table S1). The spatial relationship of RNAP relative to the ribosome is identical in NusA-NusG-TTC-B structures with mRNA spacer lengths of 10 and 13 codons, but additional EM density were found near NusA-N domain, RNAP β FTH and RNAP β' ZBD which forming an RNA binding "Curve" (Figure 4E, right panel). A ~9nt "hairpin-like" mRNA segment could be built into this density, and the mRNA segment has extensive interactions with a series of positive charged amino acids in the "Curve" (Figures S12C and S12D). Interestingly, the EM density of mRNA in the "Curve" is missing in NusA-NusG-TTC-LC structures. It suggests that the TTC-LC may transform to TTC-B by rearranging the additional ~9nt mRNA segment into the "Curve".

By using in vitro single-molecular fluorescence microscopy experiments, Qureshi and Duss demonstrates that the ribosome and RNAP can physically interact even with intervening mRNA as long as 457 nt (~147 codons)[43]. Together with our results, the TTC-LC may exit in a very wide range of mRNA lengths and be functionally important during the transcription-translation coupling.

Whole view of structural snapshots for dynamic transcription-translation coupling

In summary, our comprehensive investigation has unveiled three distinct types of TTCs, each characterized by ribosomes in various states of the translating elongation cycle. The first type, TTC-B, is formed using nucleic acid scaffolds with mRNA spacers ranging from 7 to 10. In this state, RNAP is stabilized by connecting to the ribosome 30S body via NusA and to the 30S head via NusG. This

architecture is adeptly adapted to accommodate changes in ribosome conformation throughout the translation elongation cycle, ensuring compatibility with ongoing transcription elongation. Consequently, TTC-B represents the functional, active state during the transcription-translation coupling (Figure 5). In contrast, TTC-A is obtained with nucleic acid scaffolds with most of 7 codon spacer. In TTC-A, dynamic changes in ribosome conformation during translation, particularly during mRNA translocation, would exert mechanical force on RNAP, potentially transforming the TTC-A state into TTC-B. Furthermore, with a spacer shorter than 7 codons, TTC-A may no longer be able to transform into TTC-B. In such cases, the elongating ribosome could terminate the RNAP by dissociating the mRNA from the RNAP transcription active center. Therefore, the TTC-A represents a crucial functional state within the pathway, where the ribosome engages with the halted or backtracked RNAP. This interaction can result in either the reactivation of RNAP or its termination (Figure 5). NusA-NusG-TTC-LC is obtained with nucleic acid scaffolds having mRNA spacer of 13 codons. NusA-NusG-TTC-LC is compatible with ribosome conformation changes during the translation elongation cycle and transcription elongation. We proposed that NusA-NusG-TTC-LC is the pre-coupling or post-coupling state of the transcription-translation coupling process that occurs when the ribosome is approaching the RNAP, or the RNAP is leaving away from the stalled ribosome (Figure 5).

Discussion

During transcription elongation, RNA polymerase (RNAP) adds ribonucleoside triphosphates (rNTPs) to the growing RNA chain, incorporating one rNTP per cycle[50]. During translation elongation, ribosomes use the synthesized mRNA as a template to add amino acids to the growing nascent peptide chain, incorporating one codon (three ribonucleotides) per cycle[39]. In addition, both RNAP and ribosome undergo inter-domain movements during the synthesizing cycle[31,39,40,42]. Thus, in order to coordinate the synchronization of active transcription and translation, the transcription-translation coupling process needs a very special connection between RNAP and ribosome.

Our results reveal that the interactions between RNAP and ribosome in TTC-B are relatively flexible yet within a certain range. These interactions, mediated by NusA and NusG, allow the coupling complex to adjust to the changes in ribosome tertiary structure that occur during the translation elongation cycle. Furthermore, the TTC-B contains several subclasses which differ by ~15° rotation of RNAP relative to 30S, resulting in the distance between the transcription active center and the ribosome mRNA-entrance portal changes from 79 Å, to 85 Å or 90 Å, respectively (Figures S7A and S7B). Since the average distance between two nucleotides is

~3.4Å, the difference in length between subclass1 and subclass3 is ~3-4 nt. These specific architectures enable TTC-B to accommodate 3-4 nucleotide differences in mRNA within subclasses. The similar subclasses could also be found in TTC-LC (Figure S12B). Taken together, TTC-B and TTC-LC is accommodated to the different synthesizing patterns between transcription (1nt per cycle) and translation (3nt or one codon per cycle) without disrupting their own activities. On the other hand, in TTC-A, the interactions between RNAP and ribosome are extensive tight[35-37]. In addition, in TTC-A, the mRNA moves directly from the RNAP transcription active center to the translation active site. As a result, there is less room for the mRNA to adapt to any changes during the translation elongation cycle. It is consistent with our observations that the coupling complex can hardly remain in TTC-A without experiencing any conformational changes for the later stages of the translation elongation process.

With respect to functional consequences, TTCs were noted for their role in reactivating backtracked RNAP, enhancing transcription processivity at the expense of RNA synthesis fidelity through mechanical and allosteric mechanisms[14,19,20]. Our results suggest the potential equilibrium between TTC-A and TTC-B, determined by specific codon spacer lengths, may be critical in facilitating the reactivation of backtracked RNAP during TTC. This dynamic suggests that the translating ribosome acts as a propelling force for RNAP, and upon the restart of RNAP, both the RNAP and ribosome revert to the functional TTC-B state, thereby maintaining the efficiency and integrity of the transcription-translation coupling process.

Transcription termination in bacteria is crucial for regulating gene expression, recycling RNAP, and preventing transcription-replication collisions, thereby maintaining genome stability[16,17]. Transcription in bacteria can be terminated via two primary mechanisms: intrinsic (or Rho-independent) termination, relying on the interaction of nucleic acid with RNAP, and Rho-dependent termination, mediated by the ring-shaped hexameric ATP-dependent helicase Rho[24-27]. Our molecular modeling suggests that none of these TTCs (TTC-A, TTC-B, or TTC-LC) is compatible with Rho factors involved in Rho-dependent transcription termination (Figure S13). TTC-A is also incompatible with intrinsic termination elements[35]. The findings of our study suggest that within the transcription-translation coupling complex, the ribosome can promote the termination of TEC as an alternative mechanism for transcription termination. In this scenario, the ribosome, through continuous translation in the TTC-A state, shortens the mRNA length between RNAP and the ribosome to a critical point (7 codon spacer) where the transition from TTC-A to TTC-B is not viable. We suggest the structural and mechanistic studies that involve the reactivating or terminating backtracked RNAP by the transcription-translation coupling will be facilitated by assembling the same complex as our study but

using the backtracked RNAP with mRNA spacer length of 5 or 6 codons (Figure 5).

There is another unsolved question in the study of transcription-translation coupling: The TTC-A could not be captured in vivo under normal growth conditions[51]. In our earlier work[35], TTC-A could be captured in a wide range spacer length of mRNA (5, 6, 7, and 8 codons). However, in this study, with the ribosome in a functional active state, TTC-A could only be captured within a very narrow range (major in 7 codons), and the ratio of TTC-A is also much lower. Thus, the actual ratio of TTC-A in vivo would be meager, which explains why TTC-A could hardly be captured under normal growth conditions.

Taken together, our results answer the previously open questions regarding whether transcription-translation complexes accommodate changes in ribosome throughout the translation elongation cycle; For the first time, provide a whole pictures of TTC-A, TTC-B, and TTC-LC in the process of transcription-translation coupling; suggest the potential transcription termination function by ribosome; and set the stage for, and point to the most effective approaches for, future work to define the mechanisms of reactivating or terminating backtracked RNAP by the transcription-translation coupling.

References:

1. Byrne, R., Levin, J.G., Bladen, H.A. & Nirenberg, M.W. The in Vitro Formation of a DNA-Ribosome Complex. *Proc Natl Acad Sci U S A* **52**, 140-8 (1964).

2. Miller, O.L., Jr., Hamkalo, B.A. & Thomas, C.A., Jr. Visualization of bacterial genes in action. *Science* **169**, 392-5 (1970).

3. Artsimovitch, I. Rebuilding the bridge between transcription and translation. *Molecular Microbiology* **108**, 467-472 (2018).

4. Blaha, G.M. & Wade, J.T. Transcription-Translation Coupling in Bacteria. *Annu Rev Genet* **56**, 187-205 (2022).

5. Burmann, B.M. et al. An α Helix to β Barrel Domain Switch Transforms the Transcription Factor RfaH into a Translation Factor. *Cell* **150**, 291-303 (2012).

6. Burmann, B.M. et al. A NusE:NusG Complex Links Transcription and Translation. *Science* **328**, 501-504 (2010).

7. Chatterjee, S., Chauvier, A., Dandpat, S.S., Artsimovitch, I. & Walter, N.G. A translational riboswitch coordinates nascent transcription-translation coupling. *Proceedings of the National Academy of Sciences of the United States of America* **118**(2021).

8. McGary, K. & Nudler, E. RNA polymerase and the ribosome: the close relationship. *Current Opinion in Microbiology* **16**, 112-117 (2013).

9. Proshkin, S., Rahmouni, A.R., Mironov, A. & Nudler, E. Cooperation Between Translating Ribosomes and RNA Polymerase in Transcription Elongation. *Science* **328**, 504-508 (2010).

10. Saxena, S. et al. transcription factor NusG binds to 70S ribosomes. *Molecular Microbiology* **108**, 495-504 (2018).

11. Washburn, R.S. et al. NusG Links the Lead Ribosome with the Transcription Elongation Complex. *Iscience* **23**(2020).

12. Webster, M.W. & Weixlbaumer, A. Macromolecular assemblies supporting transcription-translation coupling. *Transcription* **12**, 103-125 (2021).

13. Bailey, E.J., Gottesman, M.E. & Gonzalez, R.L. NusG-mediated Coupling of Transcription and Translation Enhances Gene Expression by Suppressing RNA Polymerase Backtracking. *Journal of Molecular Biology* **434**(2022).

14. Landick, R., Carey, J. & Yanofsky, C. Translation activates the paused transcription complex and restores transcription of the trp operon leader region. *Proc Natl Acad Sci U S A* **82**, 4663-7 (1985).

15. Peters, J.M., Vangeloff, A.D. & Landick, R. Bacterial transcription terminators: the RNA 3'-end chronicles. *J Mol Biol* **412**, 793-813 (2011).

16. Ray-Soni, A., Bellecourt, M.J. & Landick, R. Mechanisms of Bacterial Transcription Termination: All Good Things Must End. *Annu Rev Biochem* **85**, 319-47 (2016).

17. Roberts, J.W. Mechanisms of Bacterial Transcription Termination. *J Mol Biol* **431**, 4030-4039 (2019).

18. Roland, K.L., Liu, C.G. & Turnbough, C.L., Jr. Role of the ribosome in suppressing transcriptional termination at the pyrBI attenuator of Escherichia coli K-12. *Proc Natl Acad Sci U S A* **85**, 7149-53 (1988).

19. Stevenson-Jones, F., Woodgate, J., Castro-Roa, D. & Zenkin, N. Ribosome reactivates transcription by physically pushing RNA polymerase out of transcription arrest. *Proc Natl Acad Sci U S A* **117**, 8462-8467 (2020).

20. Wee, L.M. et al. A trailing ribosome speeds up RNA polymerase at the expense of transcript fidelity via force and allostery. *Cell* **186**, 1244-+ (2023).

21. Woodgate, J., Mosaei, H., Brazda, P., Stevenson-Jones, F. & Zenkin, N. Translation selectively destroys non-functional transcription complexes. *Nature* **626**, 891-896 (2024).

22. Yanofsky, C. Attenuation in the control of expression of bacterial operons. *Nature* **289**, 751-8 (1981).

23. Turnbough, C.L. Regulation of Bacterial Gene Expression by Transcription Attenuation. *Microbiology and Molecular Biology Reviews* **83**(2019).

24. Mitra, P., Ghosh, G., Hafeezunnisa, M. & Sen, R. Rho Protein: Roles and Mechanisms. *Annu Rev Microbiol* **71**, 687-709 (2017).

25. Molodtsov, V., Wang, C., Firlar, E., Kaelber, J.T. & Ebright, R.H. Structural basis of Rho-dependent transcription termination. *Nature* **614**, 367-374 (2023).

26. Richardson, J.P. Preventing the Synthesis of Unused Transcripts by Rho-Factor. *Cell* **64**, 1047-1049 (1991).

27. Zhu, M.L., Mori, M., Hwa, T. & Dai, X.F. Disruption of transcription-translation coordination in leads to premature transcriptional termination. *Nature Microbiology* **4**, 2347-2356 (2019).

28. Pelechano, V., Wei, W. & Steinmetz, L.M. Widespread Co-translational RNA Decay Reveals Ribosome Dynamics. *Cell* **161**, 1400-1412 (2015).

29. Gowrishankar, J. & Harinarayanan, R. Why is transcription coupled to translation in bacteria? *Molecular Microbiology* **54**, 598-603 (2004).

30. Artsimovitch, I. & Knauer, S.H. Ancient Transcription Factors in the News. *mBio* **10**(2019).

31. Kang, J.Y. et al. Structural Basis for Transcript Elongation Control by NusG Family Universal Regulators. *Cell* **173**, 1650-1662 e14 (2018).

32. Tomar, S.K. & Artsimovitch, I. NusG-Spt5 proteins-Universal tools for transcription modification and communication. *Chem Rev* **113**, 8604-19 (2013).

33. Werner, F. A nexus for gene expression-molecular mechanisms of Spt5 and NusG in the three domains of life. *J Mol Biol* **417**, 13-27 (2012).

34. Strauss, M. et al. Transcription is regulated by NusA:NusG interaction. *Nucleic Acids Research* **44**, 5971-5982 (2016).

35. Wang, C.Y. et al. Structural basis of transcription-translation coupling. *Science* **369**, 1359-+ (2020).

36. Kohler, R., Mooney, R.A., Mills, D.J., Landick, R. & Cramer, P. Architecture of a transcribing-translating expressome. *Science* **356**, 194-197 (2017).

37. Webster, M.W. et al. Structural basis of transcription-translation coupling and collision in bacteria. *Science* **369**, 1355-1359 (2020).

38. Molodtsov, V., Wang, C., Kaelber, J.T., Blaha, G. & Ebright, R.H. Structural basis of long-range transcription-translation coupling. *bioRxiv* (2024).

39. Carbone, C.E. et al. Time-resolved cryo-EM visualizes ribosomal translocation with EF-G and GTP. *Nature Communications* **12**(2021).

40. Frank, J. & Agrawal, R.K. A ratchet-like inter-subunit reorganization of the ribosome during translocation. *Nature* **406**, 318-22 (2000).

41. Ratje, A.H. et al. Head swivel on the ribosome facilitates translocation by means of intra-subunit tRNA hybrid sites. *Nature* **468**, 713-6 (2010).

42. Xue, L. et al. Visualizing translation dynamics at atomic detail inside a bacterial cell. *Nature* **610**, 205-+ (2022).

43. Qureshi, N. & Duss, O. Real-time tracking of transcription-translation coupling. *bioRxiv* (2023).

44. Loveland, A.B., Demo, G. & Korostelev, A.A. Cryo-EM of elongating ribosome with EF-Tu•GTP elucidates tRNA proofreading. *Nature* **584**, 640-+ (2020).

45. Ermolenko, D.N. et al. The antibiotic viomycin traps the ribosome in an intermediate state of translocation. *Nature Structural & Molecular Biology* **14**, 493-497 (2007).

46. Zhang, L. et al. The structural basis for inhibition of ribosomal translocation by viomycin. *Proceedings of the National Academy of Sciences of the United States of America* **117**, 10271-10277 (2020).

47. Zhou, J., Lancaster, L., Donohue, J.P. & Noller, H.F. Crystal Structures of EF-G-Ribosome Complexes Trapped in Intermediate States of Translocation. *Science* **340**, 1543-+ (2013).

48. Fernández, I.S. et al. Unusual base pairing during the decoding of a stop codon by the ribosome. *Nature* **500**, 107-U136 (2013).

49. Zhou, J., Lancaster, L., Donohue, J.P. & Noller, H.F. How the ribosome hands the A-site tRNA to the P site during EF-G-catalyzed translocation. *Science* **345**, 1188-1191 (2014).

50. Li, L.T., Molodtsov, V., Lin, W., Ebright, R.H. & Zhang, Y. RNA extension drives a stepwise displacement of an initiation-factor structural module in initial transcription. *Proceedings of the National Academy of Sciences of the United States of America* **117**, 5801-5809 (2020).

51. O'Reilly, F.J. et al. In-cell architecture of an actively transcribing-translating expressome. *Science* **369**, 554-+ (2020).

Figures legends:

Figure 1. Structure determination: transcription-translation complexes (TTCs)

(A) Nucleic-acid scaffolds. Each scaffold comprises nontemplate- (gray) and template-strand (blue) oligodeoxyribonucleotides and one of seven oligoribonucleotides (red), corresponding to mRNA. Dashed black box labeled "TEC" represents a portion of nucleic-acid scaffold that forms TEC upon the addition of RNAP. It includes a 10 nt nontemplate- and template-strand ssDNA segments forming "transcription bubble", a 9 nt of mRNA engaged with the template-strand DNA as RNA-DNA "hybrid", and 5 nt of mRNA, on diagonal, in the RNAP RNA-exit channel. The orange line labeled "Met" represents the mRNA AUG codon intended to occupy ribosome P site upon the addition of ribosome and fMet-tRNA^{fMet}. The dark green lines labeled “Phe” represents mRNA UUU codon intended to occupy ribosome A site upon addition of Phe-tRNA^{Phe}, The purple line labeled “Leu” represents mRNA CUU codon.The "spacer" denotes mRNA length between the TEC and the initiation codon AUG counted by codons.

(B) Schematic of active TTCs reconstitution. In the first step (left panel), RNAP core in complex with nucleic acid scaffold forms TEC. In the second step (second panel), TEC binds with ribosome 70S through NusA and NusG bridging, and mRNA AUG codon pairs with anticodon of fMet-tRNA^{fMet} in the P site of 30S ribosomal subunit. In the third step (third panel), the EF-Tu ternary complex delivers Phe-tRNA^{Phe} into the decoding center on 30S ribosomal subunit. In the fourth step (right panel), EF-G motivates translocation of mRNA and paired tRNAs. RNAP in TEC is represented in gray, non-template strand DNA, template strand DNA, and RNA are in black, blue, and red, respectively. The codons AUG, UUU, and CUU are in orange, green, and purple, respectively. The non-rotated 30S subunit is shown in yellow, rotated 30S subunit in wheat, and 50S subunit in dark gray. NusA is shown in light blue, NusG in magenta, fMet-tRNA^{fMet} in orange, Phe-tRNA^{Phe} in forest, and EF-G in cyan.

Figure 2. Cryo-EM structures of NusA-NusG-TTC-B

(A) Side view of the TTC-B model layered on the top of cryoEM maps. The five representative panel, from left to right, are TTC-B in state1 at 4.5 Å resolution (n = 9), state2 at 4.9 Å (n = 9), state3 at 5.2 Å (n = 10), state4 at 4.9 Å (n = 9), and state5 at 4.6 Å (n = 9), respectively. Color-coding is the same as in Figure 1, except when stated differently. Ribosome stalk is omitted for clarity in this and all subsequent images.

(B) Close-up view of mRNA connecting the RNAP active center and the tRNA channel in the five TTC-B states. The cryoEM map is represented by blue mesh. The disordered mRNA nucleotides indicated by dashed lines. RNAP

active-center catalytic Mg^{2+} in purple sphere. Three rectangles with dashed lines indicate A/P/E site in the ribosome.

(C) Structure comparison of TTC-B state1 and state2 by superposition of 50S subunit. Top view from mRNA entry channel of 30S subunit (left panel) and orthogonal view orientation showing the movement of RNAP and 30S subunit (right panel). The 16S rRNA in TTC-B is shown in yellow ribbon for state1 and wheat for state 2. The RNAP is shown in gray surface for state1 and cyan for state2. The NusA is shown in blue and NusG magenta with state 1 distingished with transparency. The superposition reveals a 11.3^{o} counterclockwise rotation of NusG (magenta arrow) and a 2.2^{o} counterclockwise rotation of NusA (blue arrow).

(D) Comparison of TTC-B state1 to 5 based on 30S subunit superimposition. Color code as in Figure 2A with states 2-4 in more transparent colors.

(E) (F) Close-up view of points flexibility in NusA and NusG. Flexible linkages in NusA (NTD-S1 linker, AR1-KH2 linker, AR1-AR2 linker; dashed line circle) and flexible NusG bridging of RNAP and ribosome (NusG linker; dashed line circle). Colors as in Figure 2A with state2-4 in more transparent colors.

Figure 3. Cryo-EM structures of TTC-A

(A) Cryo-EM structures of TTC-A obtained using mRNA with codon spacer of 7 and 9. Structures shown are TTC-A state2 at 7.0 Å resolution (n = 9) and state3 at 4.6 Å (n = 7). Views and colors are the same as in Figure 2A. Absence density in TTC-A state 3 is indicated by a dashed oval.

(B) Closeup view of mRNA connecting the RNAP active center and the tRNA channel in two states of TTC-A. Views and colors are same as in Figure 2B.

(C) Comparison of TTC-A state 2 and 3 by superimpose on 30S subunit. The 16S rRNA of 30S subunit in TTC-A is shown in yellow. The ribosomal protein uS3, uS4 and uS10 interacting with RNAP are highlighted in orange, dark green, and red, respectively. Superposition reveals a 4.1^{o} rotation and 2.1 Å translation between RNAP in state2 (white surface) and RNAP in state3 (light cyan surface), as illustrated by black arrows.

(D) Absence of EM density for RNAP β' ZBD domain in TTC-A state3. EM density is represented by blue mesh. Atomic models for RNAP β' and uS4 are shown in pink and dark green ribbon, respectively. The location of missing EM density for β' ZBD is indicated by a dashed oval. The β' ZBD in TEC in the absence of ribosome (TTC-A state2) is shown in white ribbon.

(E) Absence of EM density for parts of RNAP αI domain in TTC-A state3. The cryoEM map is rerpresented by

blue mesh. The atomic models for RNAP αI and uS10 is shown in light green and red ribbon, respectively. The missing cryoEM map for parts of RNAP αI is indicated by dashed oval. The αI in TEC (TTC-A state2) is shown as white ribbon.

(F) Distribution of TTC-A and TTC-B in different spacer length. Upper panel: distribution of TTC-A and TTC-B in "translational static state" with spacer lengths of 5, 6, 7, 8, 9, or 10 codons; lower panel: distribution of TTC-A and TTC-B in "translational translocation states" TTCs with spacer lengths of 5, 6, 7, 8, 9, or 10 codons.

(G) Cryo-EM structures of "de-coupled" ribosome obtained using mRNA with codon spacer of 5 to 6. Views and colors are as in Figure 2A. Cryo-EM maps (gray surface) and fit (brick-red ribbons) for prematurely terminated mRNA are illustrated by black arrow.

Figure 4. Cryo-EM structure of NusA-NusG-TTC-LC

(A) Cryo-EM structures of NusA-NusG-TTC-B and NusA-NusG-TTC-LC (obtained with spacer lengths of 13 codons). Structures shown are NusA-NusG-TTC-B state1 (4.6 Å; n = 13; Table S1), NusA-NusG-TTC-LC state1 (4.6 Å; n = 13; Table S1), NusA-NusG-TTC-LC state3 (5.1 Å; n = 13; Table S1), Views and colors as in Figure 2A.

(B) RNAP-NusG interactions involving RNAP β' ZBD and NusG (subpanel 1) and RNAP-NusA interactions involving RNAP β' ZBD and NusA (subpanel 2). mRNA-NusA interactions involving mRNA and NusA-KH1 domain (subpanel 3) and mRNA-ribosome interactions involving mRNA and ribosomal protein S3 (subpanel 4).

(C) Structure comparison of NusA-NusG-TTC-LC state1 and state3 by superposition of 50S subunit. Views and colors as in Figure 2C. Top view from mRNA entry channel of 30S subunit (left panel) and orthogonal view orientation showing the movement of RNAP and 30S subunit (right panel). The 16S rRNA in TTC-LC is shown in yellow ribbon for state1 and wheat for state 3. The RNAP is shown in gray surface for state1 and cyan for state3. The NusA is shown in blue and NusG magenta with state 1 distingished with transparency. The superposition reveals a 10.9^{o} counterclockwise rotation of NusG (magenta arrow) and a 7.1^{o} counterclockwise rotation of NusA (blue arrow).

(D) Comparison of NusA-NusG-TTC-LC state1 to NusA-NusG-TTC-B state1, superposition on 30S. Colors as in Figure 2D with NusA-NusG-TTC-B state1 in more transparent color.

(E) Comparison of mRNA extending in NusA-NusG-TTC-B state1 (obtained with spacer lengths of 10 or 13 codons). EM density map of mRNA near the RNAP mRNA exit channel in NusA-NusG-TTC-B state1 with mRNA spacer length of 10 codons, atom models of NusA-NTD and S1 domains, RNAP β FTH, RNAP β ZBD are shown in light blue, cyan, and pink, respectively (left panel). EM density map of mRNA near the RNAP mRNA exit channel in NusA-NusG-TTC-B state1 with mRNA spacer length of 13 codons (right panel), views and colors as left panel.

Figure 5. Schematic depiction of proposed transcription-translation coupling throughout translation elongation cycle. With a mRNA codon spacer length of 7 to 10, the TTCs are in TTC-B state. Ribosome throughout various of translation stages, including “pre-translocation” ribosome in state 1, “translocation intermediate” in state 2 to 4 and “post-translocation” in state 5. The RNAP in TTC-B remains stable with the ribosome due to NusA and NusG bridging both of them. With mRNA spacer lengths of 7, 8, and 9, the TTCs could also being in TTC-A state. A state is incompatible for ribosome pass through the translation elongation cycle but could transformed into TTC-B. With mRNA spacer length shorther than 6 (including 6 codons), TTCs cannot be formed, and the TEC is terminated by ribosome. With mRNA spacer length longer than 13 codons (including 13 codons), the TTCs are in NusA-NusG-TTC-LC state. The RNAP in this state is also bridging by NusA, NusG with ribosome, but is less stable during the translation elongation cycle. With mRNA spacer length of 13 codons, TTC-LC and TTC-B could transform to each other. Components used in models are further explained in the lower panel. The models with dashed line are not determined in our work.

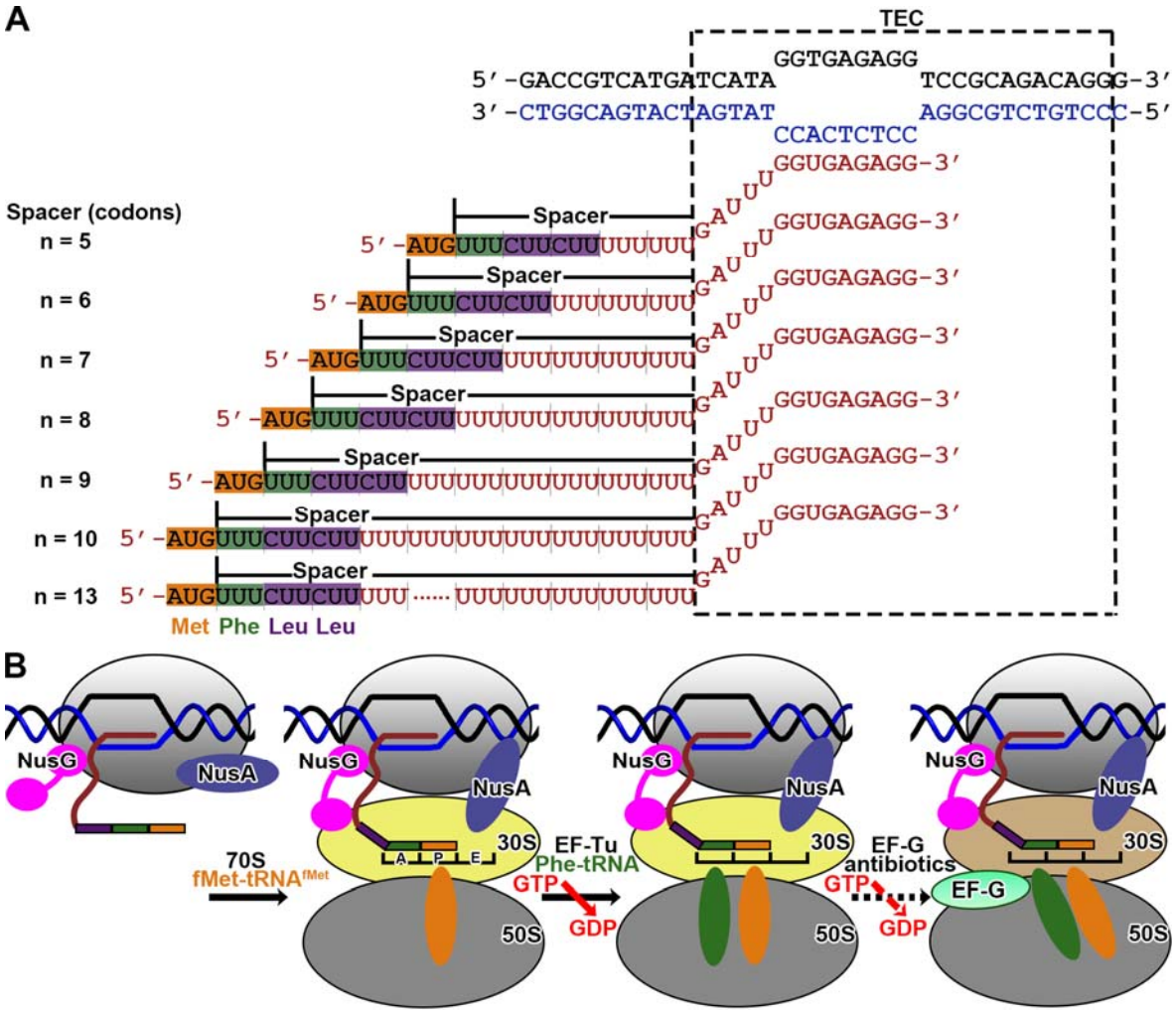
A
TEC
GGTGAGAGG
5′-GACCGTCATGATCATA
TCCGCAGACAGGG-3′
3′-CTGGCAGTACTAGTAT
AGGCGTCTGTCCC-5′
CCACTCTCC
GGUGAGAGG-3′
Spacer (codons)
n = 5
n = 6
n = 7
n = 8
n = 9
n = 10
n = 13
Spacer
5′-AUGUUUCUUCUUUUUUUU
5′-AUGUUUCUUCUUUUUUUUUU
5′-AUGUUUCUUCUUUUUUUUUUUU
5′-AUGUUUCUUCUUUUUUUUUUUUUU
5′-AUGUUUCUUCUUUUUUUUUUUUUUUU
5′-AUGUUUCUUCUUUUUUUUUUUUUUUUUU
5′-AUGUUUCUUCUUUUUUUUUUUUUUUUUUUU
Met Phe Leu Leu
B
NusG
NusA
70S
fMet-tRNAfMet
30S
50S
A
P
E
EF-Tu
Phe-tRNA
GTP
GDP
EF-G
antibiotics
EF-G

Figure 1

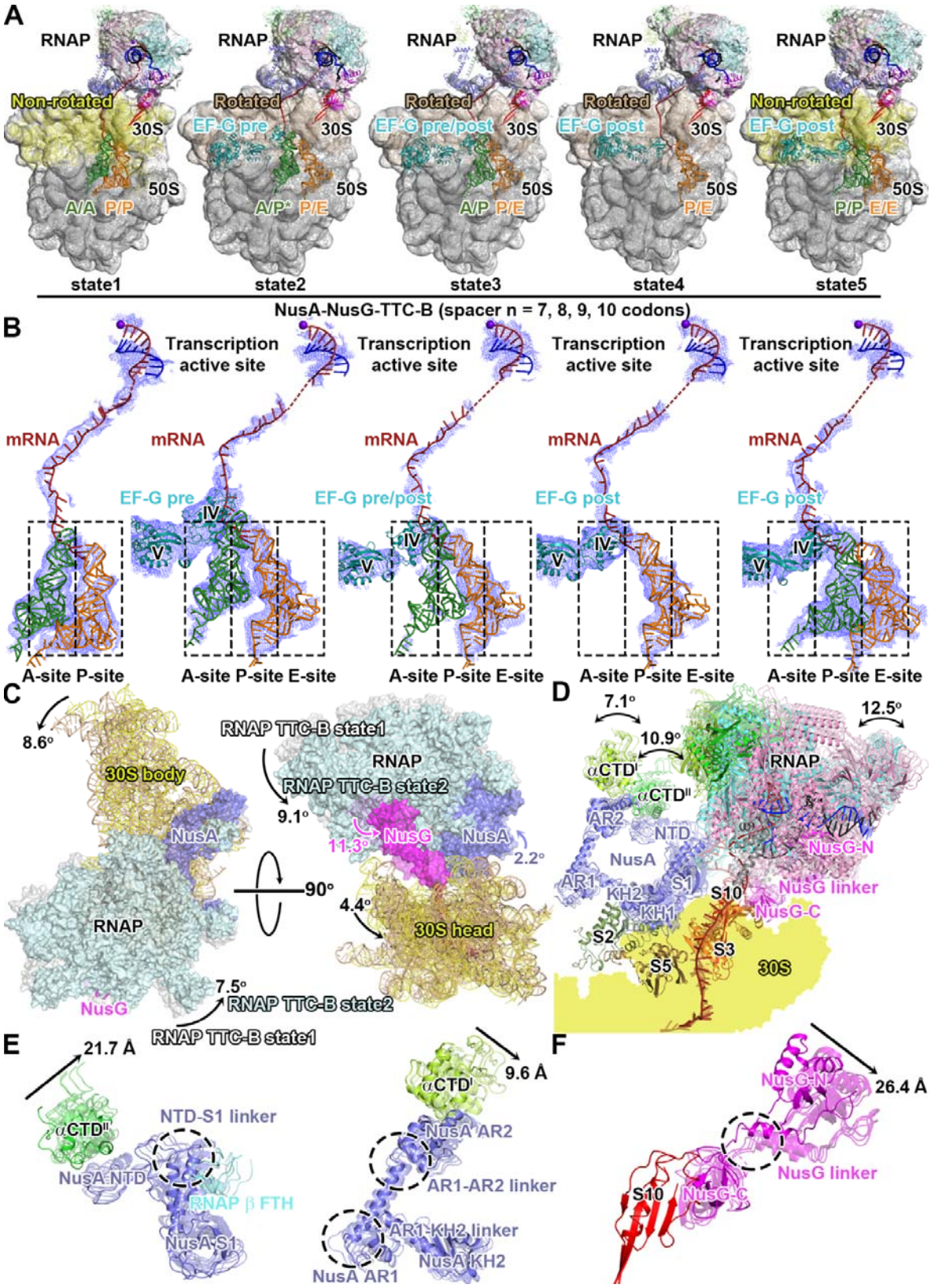
A
RNAP
Non-rotated
30S
50S
A/A P/P
state1
Rotated
EF-G pre
A/P* P/E
state2
EF-G pre/post
A/P P/E
state3
EF-G post
P/E
state4
EF-G post
P/P E/E
state5
NusA-NusG-TTC-B (spacer n = 7, 8, 9, 10 codons)
B
Transcription active site
mRNA
EF-G pre
EF-G pre/post
EF-G post
IV
V
A-site P-site
A-site P-site E-site
C
8.6°
30S body
NusA
RNAP
NusG
RNAP TTC-B state1
RNAP TTC-B state2
9.1°
11.3°
2.2°
90°
4.4°
30S head
7.5°
D
7.1°
10.9°
12.5°
αCTD'
αCTD''
AR2
NTD
NusA
AR1
KH2
KH1
S1
S2
S3
S5
S10
NusG-N
NusG linker
NusG-C
30S
E
21.7 Å
αCTD''
NTD-S1 linker
NusA NTD
RNAP β FTH
NusA S1
9.6 Å
αCTD'
NusA AR2
AR1-AR2 linker
AR1-KH2 linker
NusA KH2
NusA AR1
F
26.4 Å
NusG-N
NusG linker
S10
NusG-C

Figure 2

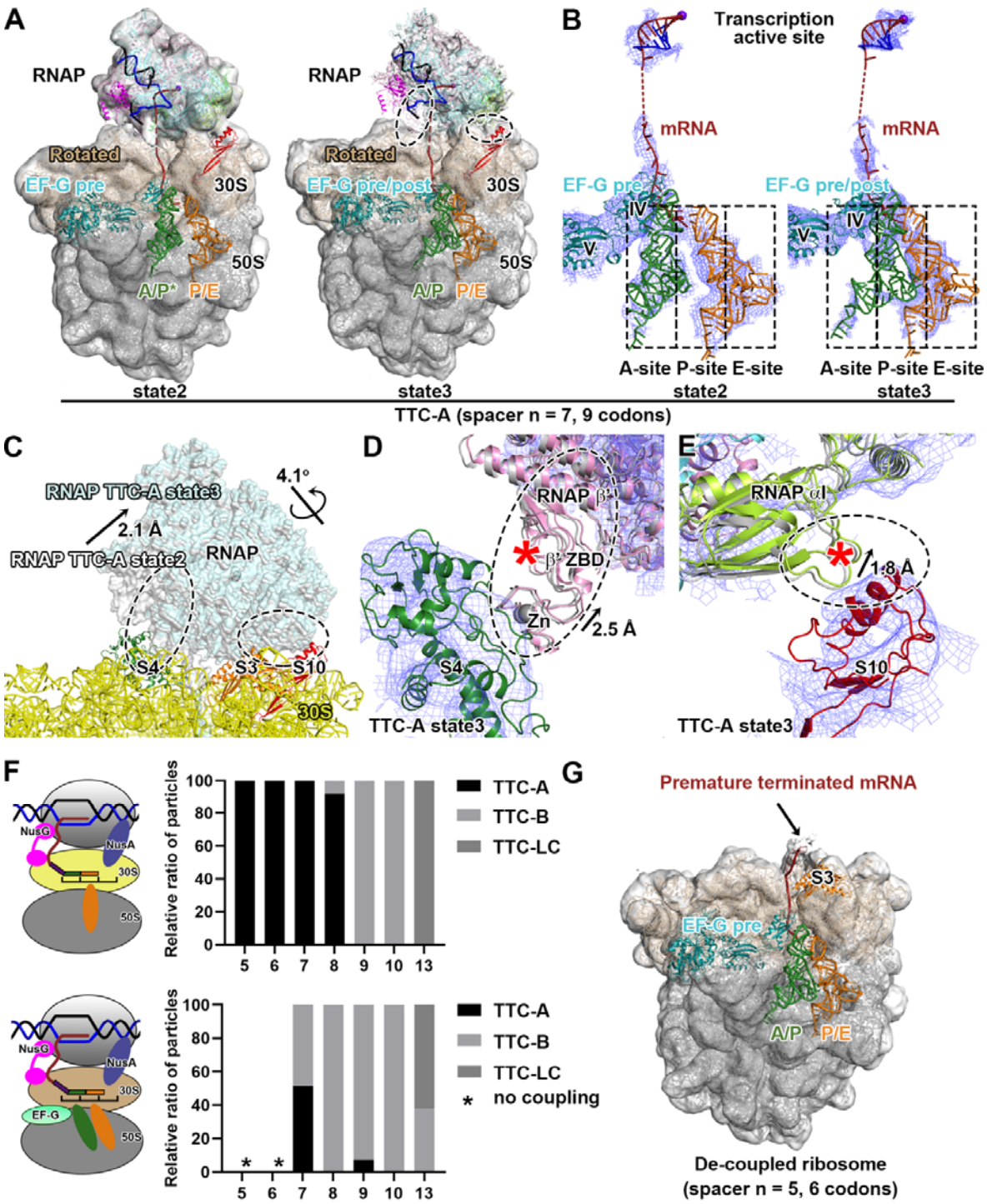
A
RNAP
Rotated
EF-G pre
30S
50S
A/P*
P/E
state2
RNAP
Rotated
EF-G pre/post
30S
50S
A/P
P/E
state3
B
Transcription active site
mRNA
EF-G pre
IV
V
A-site P-site E-site
state2
mRNA
EF-G pre/post
IV
V
A-site P-site E-site
state3
TTC-A (spacer n = 7, 9 codons)
C
RNAP TTC-A state3
4.1°
2.1 Å
RNAP TTC-A state2
RNAP
S4
S3
S10
30S
D
RNAP β'
β' ZBD
Zn
2.5 Å
S4
TTC-A state3
E
RNAP αI
1.8 Å
S10
TTC-A state3
F
NusG
NusA
30S
50S
Relative ratio of particles
100
80
60
40
20
0
5
6
7
8
9
10
13
TTC-A
TTC-B
TTC-LC
NusG
NusA
30S
EF-G
50S
Relative ratio of particles
TTC-A
TTC-B
TTC-LC
* no coupling
G
Premature terminated mRNA
S3
EF-G pre
A/P
P/E
De-coupled ribosome
(spacer n = 5, 6 codons)

Figure 3

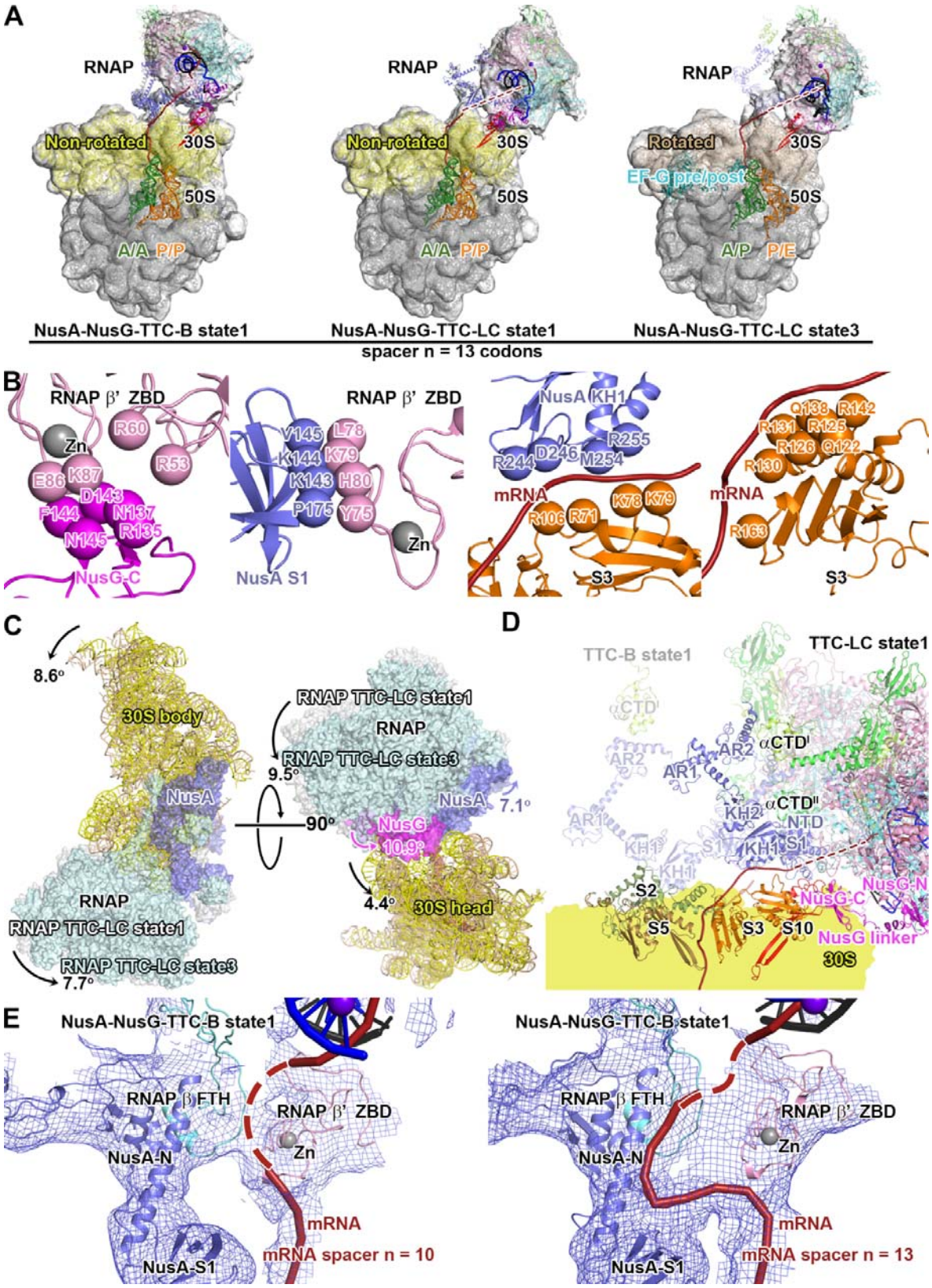
A
RNAP
Non-rotated
30S
50S
A/A P/P
NusA-NusG-TTC-B state1
RNAP
Non-rotated
30S
50S
A/A P/P
NusA-NusG-TTC-LC state1
RNAP
Rotated
30S
EF-G pre/post
50S
A/P P/E
NusA-NusG-TTC-LC state3
spacer n = 13 codons
B
RNAP β' ZBD
Zn
R60
R53
E86
K87
D143
F144
N137
R135
N145
NusG-C
RNAP β' ZBD
V145
L78
K144
K79
K143
H80
P175
Y75
Zn
NusA S1
NusA KH1
R255
R244
D246
M254
mRNA
R106
R71
K78
K79
S3
Q138
R142
R131
R125
R126
Q122
R130
mRNA
R163
S3
C
8.6°
30S body
NusA
RNAP
RNAP TTC-LC state1
RNAP TTC-LC state3
7.7°
RNAP TTC-LC state1
RNAP
RNAP TTC-LC state3
9.5°
90°
NusA
7.1°
NusG
10.9°
4.4°
30S head
D
TTC-B state1
TTC-LC state1
αCTD
AR2
AR1
αCTD
KH2
αCTD
NTD
KH1
S1
S2
S5
S3
S10
NusG-N
NusG-C
NusG linker
30S
E
NusA-NusG-TTC-B state1
RNAP β FTH
RNAP β' ZBD
Zn
NusA-N
mRNA
NusA-S1
mRNA spacer n = 10
NusA-NusG-TTC-B state1
RNAP β FTH
RNAP β' ZBD
Zn
NusA-N
mRNA
NusA-S1
mRNA spacer n = 13

Figure 4

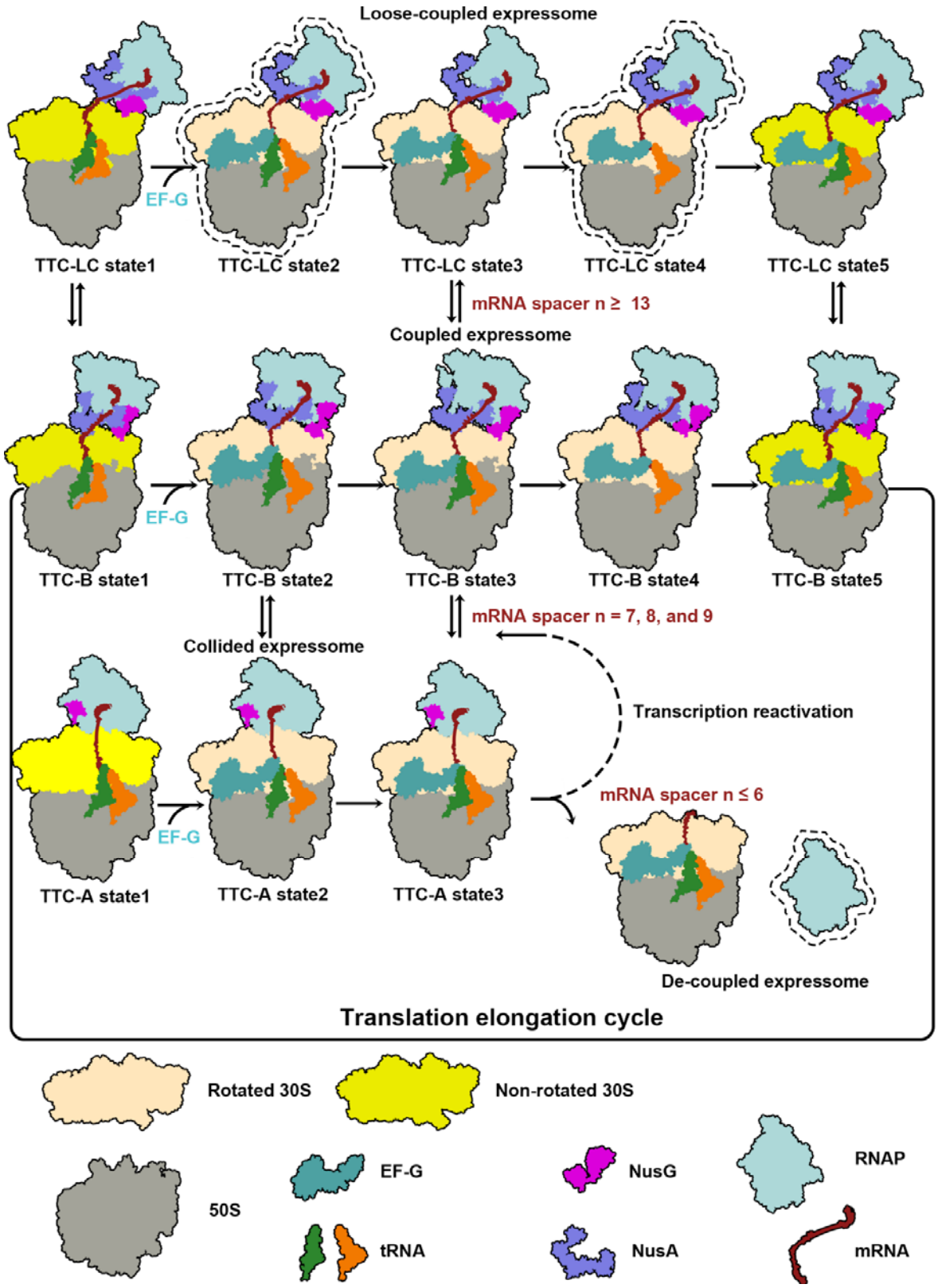
Loose-coupled expressome
EF-G
TTC-LC state1
TTC-LC state2
TTC-LC state3
TTC-LC state4
TTC-LC state5
mRNA spacer n ≥ 13
Coupled expressome
EF-G
TTC-B state1
TTC-B state2
TTC-B state3
TTC-B state4
TTC-B state5
mRNA spacer n = 7, 8, and 9
Collided expressome
Transcription reactivation
mRNA spacer n ≤ 6
EF-G
TTC-A state1
TTC-A state2
TTC-A state3
De-coupled expressome
Translation elongation cycle
Rotated 30S
Non-rotated 30S
50S
EF-G
NusG
RNAP
tRNA
NusA
mRNA

Figure 5